Two-proton transfer reactions on even Ni and Zn isotopes

A. Boucenna,* L. Kraus, and I. Linck
Centre de Recherches Nucléaires, F-67037 Strasbourg CEDEX, France

Tsan Ung Chan
Institut des Sciences Nucléaires, F-38026 Grenoble CEDEX, France
(Received 29 December 1988)

New levels strongly excited by 112-MeV ^{12}C ions on even Ni and Zn isotopes are J^π assigned on kinematical and geometrical arguments, crude shell-model calculations, and distorted-wave Born approximation angular-distribution analysis. These tentative assignments are supported by the Bansal-French model. Because of the contribution of additional collective effects, the two-proton transfer reaction spectra are less selectively fed than those obtained with the analogous two-neutron transfer reactions induced on the same targets in a similar energy range.

I. INTRODUCTION

Most of the high-spin states[1] in f-p shell nuclei have been observed by in-beam spectroscopy using fusion-evaporation reactions. These reactions feed only yrast or quasiyrast states that can have many different configurations. On the other hand, transfer reactions are very selective and favor the population of states with a particular configuration.[2–7] The comparison of results from these two kinds of reactions for the same residual nucleus can shed light on the assignment of J^π and/or the level configurations.

Obviously the $g_{9/2}$ shell plays an important role in the explanation of high-spin states in the heaviest f-p nuclei,[5,6,8] but due to the large size of the involved matrix complete shell-model calculations are scarce. The crude shell model[9] (CSM), which considers two nucleons moving around an inert target core, predicts the energy of high-spin states formed by two nucleon transfers as the sum of the excitation energies of the corresponding single-particle levels plus (when the two transferred nucleons are identical) an easily calculable pairing energy. Thus the 7^- and 8^+ yrast states in the even isotopes of Zn and Ge have been established as $2n$ states.[9] Similarly, the results of (α,^{2}He) reaction studies[5,6] on Fe, Ni, Zn, and Ge isotopes agree with the predictions of the CSM.[9,10]

The 7^- and 8^+ two-proton high-spin states, unobserved up to now, are expected in these nuclei above the similar $2n$ configuration states.[10] In order to form these states with a maximum cross section, we have performed (^{12}C, ^{10}Be) reactions on Ni and Zn isotopes at an incident energy favoring the transfer of angular momentum that best matches the large angular momentum difference between the grazing waves in the entrance and exit channels. The most important newly observed peaks have been J^π assigned according to $2p$ cluster selection rules, CSM predictions,[10] and angular distribution DWBA analysis. The results are compared with Bansal-French model predictions.[11] Among the residual nuclei studied, ^{66}Zn is of particular interest since it can be formed with $2n$ and $2p$ transfer reactions on ^{64}Zn and ^{64}Ni targets, respectively. The relative population of states in both reactions will help to distinguish between $2n$ and $2p$ states.

Population of states appears less selective in the (^{12}C, ^{10}Be) $2p$ transfer reactions than in the $2n$ transfers. This is explained by additional collective effects in the final nuclei that have been taken into account in a semiphenomenological model[12] that considers the coupling of two quasiparticles to a triaxial Davidov rotor in a space including $N=4$ $g_{9/2}$ neutron and proton levels.

II. EXPERIMENTAL PROCEDURE

A beam of 112-MeV $^{12}C^{6+}$ was provided by the Strasbourg MP accelerator. Typical beam currents were 50 electrical nA. Targets of self-supporting Ni foils between 80 and 180 μg/cm^2 thick, and Zn foils between 85 and 228 μg/cm^2 thick on 20-μg/cm^2 C backings. These thicknesses have been determined to about 10% with an α-particle gauge. The isotopic enrichments of the ^{58,60,62,64}Ni were 99.89, 99, 97.94, and 98.02 % and of the ^{64,66,68}Zn 99.4, 99, and 98.9 %, respectively.

Ejectiles were momentum analyzed in a 5- or 10-msr solid angle with a three dipoles and one quadrupole (Q3D) spectrometer ($dp/p = 2.10^{-4}$) coupled to the incident beam in an energy-loss mode. A gaseous hybrid counter composed of three proportional counters separated by two ionization chambers of 4- and 15-cm depth was placed along the focal plane at an angle of 45° to the propagation direction of the detected particles. Two 13-μm Mylar foils separated the isobutane of the counter (100–150 Torr) from the vacuum of the detection chamber, while allowing the particles to reach a 2-cm-thick NE110 scintillator.

The ejectiles, detected in the 11% momentum acceptance of the counter, were identified by their energy loss ΔE in the ionization chambers and residual energy E_R in the scintillator. Correction of the ΔE spectra for entrance angle in the 6° opening of the spectrometer resulted in good mass separation of the detected ejectiles. Position spectra in the first and third proportional counters, separated by 211.5 mm, were obtained by charge division. Conditioned by the ΔE and E_R requirements, the positions allowed reconstruction of the trajectories of the studied ejectiles, the determination of the particle entrance angle, and construction of momentum spectra on the focal plane. The overall resolution was 100–200 keV.

III. ANALYSIS PROCEDURE

To analyze the $2p$ transfer spectra producing Zn and Ge isotopes we take into account two-nucleon aspects and collective aspects that coexist in these final nuclei.

A. Two-nucleon aspects

1. Semiclassical selection rules

The transfer of a ($T=1$, $S=0$) $2p$ cluster on a 0^+-target nucleus leads to final states of natural parity and takes place with a large probability when three kinematical conditions, established by Brink, are satisfied within reasonable limits[13]

$$\Delta k R_2 = |k_0 R_2 - M_{L_2} - (R_2/R_1) M_{L_1}| \le 2\pi R_2/R \ , \quad (1)$$

$$\Delta L = |M_{L_2} - M_{L_1} + k_0(R_1 - R_2)/2 + Q_{\rm eff} R/\hbar v \le 2 \ , \quad (2)$$

$$L_1 + M_{L_1} = \text{even}, \quad L_2 + M_{L_2} = \text{even} \ . \quad (3)$$

L_1, M_{L_1} and L_2, M_{L_2} are the orbital momenta of the transferred cluster and their z projections in the initial and final nuclei, $k_0 = mv/\hbar$, m is the mass of the transferred cluster, and v is the relative velocity of the two nuclei. R_1 and R_2 are the radii of the projectile and target nuclei,

$$R = R_1 + R_2 \ ,$$

$$Q_{\rm eff} = (Q - Z_1^f Z_2^f - Z_1^i Z_2^i) e^2/R \ ,$$

where Q is the reaction Q value and $Z_1^f, Z_2^f, Z_1^i, Z_2^i$, the nuclei charges in the initial and final channel. For all reactions considered here $k_0 R_2$ is large (Table I) and final states with large orbital momenta will be favored. Table I gives the values of M_{L_2} and L_2 deduced from Eqs. (1), (2), and (3). In this table the expected orbits favored by these kinematical conditions in the final nuclei are also mentioned.

The total transition probability[3] depends on the three kinematical conditions and contains the Clebsch-Gordan coefficients of the angular momentum coupling of the cluster in the initial and final nuclei. It is shown (Fig. 1) that for ^{60}Zn, for example, the probability of exciting states with spins in the range 4–8 is much greater than for lower spin values when these states are formed by $2p$ transfer induced by 112-MeV ^{12}C ions, on a 0–10 MeV excitation energy range. Therefore $J^+ = 6^+$, 7^-, and 8^+ states should be well populated.

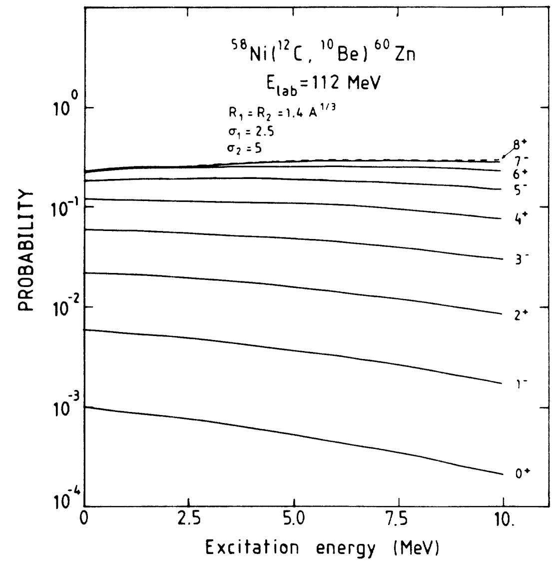

FIG. 1. Total transition probability of a $2p$-cluster transfer on ^{58}Ni versus the excitation energy and the J^π value of the final states in the semiclassical model of Brink [Eq. (4.15) of Ref. 3].

TABLE I. Favored two-proton stripping orbits at 112-MeV ^{12}C incident energy.

Reactions	Q_0 (MeV)	$k_0 R_2$ ($\hbar$)	L_1 ($\hbar$)	M_{L_1} ($\hbar$)	M_{L_2} ($\hbar$)	L_2 ($\hbar$)	Favored orbits
^{58}Ni(^{12}C,^{10}Be)^{60}Zn	−18.65	6.44	0	0	4–8	48	d,f,g
^{60}Ni(^{12}C,^{10}Be)^{62}Zn	−15.91	6.51	0	0	4–7	4–7	d,f,g
^{62}Ni(^{12}C,^{10}Be)^{64}Zn	−13.35	6.58	0	0	4–6	4–6	d,f
^{64}Ni(^{12}C,^{10}Be)^{66}Zn	−10.81	6.65	0	0	4–6	4–6	d,f
^{64}Zn(^{12}C,^{10}Be)^{66}Ge	−16.98	6.65	0	0	4–7	4–7	d,f,g
^{66}Zn(^{12}C,^{10}Be)^{68}Ge	−14.53	6.72	0	0	4–7	4–7	d,f,g
^{68}Zn(^{12}C,^{10}Be)^{70}Ge	−12.05	6.79	0	0	4–6	4–6	d,f
^{58}Ni(^{12}C,^{10}C)^{60}Ni	−11.45	6.43	0	0	4–8	4–8	d,f,g
^{60}Ni(^{12}C,^{10}C)^{62}Ni	−13.42	6.50	0	0	4–8	4–8	d,f,g
^{62}Ni(^{12}C,^{10}C)^{64}Ni	−15.35	6.57	0	0	4–9	4–9	d,f,g
^{64}Ni(^{12}C,^{10}C)^{66}Ni	−16.54	6.64	0	0	4–9	4–9	d,f,g
^{64}Zn(^{12}C,^{10}C)^{66}Zn	−12.80	6.64	0	0	4–9	4–9	d,f,g

2. *Two-proton transfer spectroscopic factor*

The two-proton transfer spectroscopic factor is proportional to the overlap of the wave functions of the two transferred nucleon relative motion and of the 0*s* cluster. Figure 2 shows this overlap function versus the total spin J for several configurations.[14] It is observed that the wave functions of the states with spins coupled to their maximum, have large overlap with the 0*s* cluster wave function. For instance, states of configuration $(1g_{9/2})^2_{8+}$ are expected to be fed very selectively.

The fit of the angular distributions by distorted-wave Born approximation (DWBA) calculations allows us to determine the relative spectroscopy factor α for different final states of a nucleus.

3. *Shell-model calculations*

The great selectivity of two-nucleon stripping reactions results in the preferential excitation of high-spin states of rather simple configuration.[2] Thus, simple shell-model calculations have been performed to try to explain them, particularly for $J=0^+$, $T_z=0$ target nuclei. When two nucleons are transferred to the orbits j_1 and j_2 outside the core A_0, the excitation energy in the final nuclear state (J,T) is given[15] by

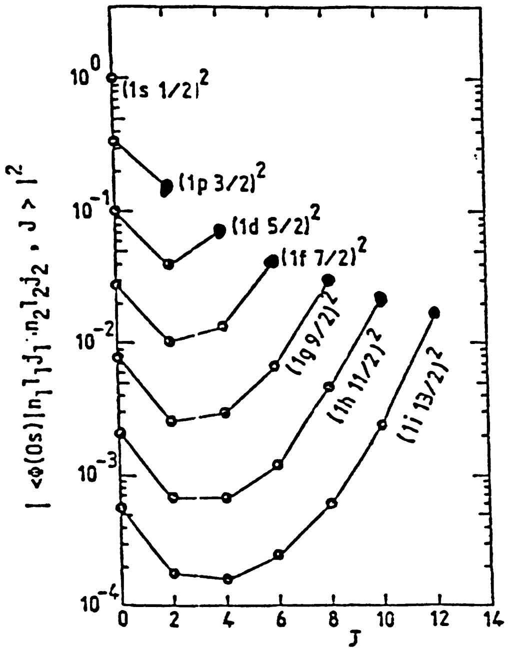

FIG. 2. Overlap of the wave functions of the 0*s* cluster and the two transferred proton relative motion versus total spin J.

$$E^*(A_0+N+N',j_1,j_2,J,T)=E_B(A_0,\text{g.s.})-E_B(A_0+N+N',\text{g.s.})+\epsilon(j_1)+\epsilon(j_2)+E_c+\langle j_1j_2|V|j_1j_2\rangle_{JT} \tag{4}$$

TABLE II. Excitation energy, spin, and parity of ^{66}Zn levels.

Previous works			Present work					
E_x (MeV)	J^π	Band[d]	E_x (MeV)	$d\sigma/d\omega$[e] (μb/sr)	Configuration	CSM (MeV)	J^{π}[f]	
0.000[a,b]	0	g.s.	0.0					
1.039[a,b]	2^+	g.s.	1.04	73				
1.873[a,b]	2^+		1.89					
2.450[a,b]	4^+	g.s.	2.47					
2.827[a,b]	3^-	NP	2.84	172				
3.077[a,b]	4^+		3.06	245	$(\pi f_{5/2})^2_{4^+}$	3.703		
3.746[a]	5^-	NP	3.74	210	$(\pi p_{3/2}\pi g_{9/2})_{5^-}$	4.007		
4.182[a]	(6^+)	g.s.						
			4.20	292				
4.251[a,c]	(7^-)	NP			$(\nu f_{5/2}\nu g_{9/2})_{7^-}$	4.146	7^-	*S*
4.814[a]	(7^-)		4.80	125				
					$(\pi f_{5/2}\pi g_{9/2})^{7^-}$	5.122	(7^-)	*S,T*
5.207[a,c]	(8^+)	g.s.	5.20	284	$(\nu g_{9/2})^2_{8^+}$	5.211	8^+	*S*
5.464[a]	(9^-)	NP	5.40					
			5.60					
5.74[c]	(6^+)							
			6.00					
			6.85	196	$(\pi g_{9/2})^2_{8^+}$	6.541	(8^+)	*S,T*
			7.55	180	$(\pi g_{9/2}\pi d_{5/2})_{6^+}$	(7.398)	(6^+)	*S,T*

[a]Reference 19.
[b]Reference 20.
[c]Reference 6.
[d]Reference 21.
[e]Cross section at $\theta_{\text{lab}}=10°$ with an absolute error of 30%.
[f]Spin and parity assignments at the right in the table are based on systematic trends *S* and on crude shell-model (CSM) calculations *T*.

where the E_B terms are experimental binding energies[16] (taken to be negative), E_c is the Coulomb interaction energy, and $\epsilon(j)$ are the single-particle energies

$$\epsilon(j)=E_B(A_0+1,j)-E_B(A_0,\text{g.s.}) ,$$

with

$$E_B(A_0+1,j)=E_B(A_0+1,\text{g.s.})+E^*(A_0+1,j) .$$

The last term in Eq. (4), which is the two-body matrix element (TBME), describing the interaction between active particles outside the core, has been calculated[17] or experimentally estimated.[6] It is generally weak for the configurations considered in this work. In our calculations done in the crude shell-model approximation[9,10] the TBME and the Coulomb energy terms have been neglected. The positions of the aligned configuration high-spin states corresponding to the filling of the available empty shells of the target nuclei ($f_{5/2}$, $g_{9/2}$, and $2d_{5/2}$ shells) reported in Tables II–VIII (CSM column), have been calculated from recent mass value[16] and single-particle energies reported in Table IX.

B. Collective aspects

Previous experimental work has shown that prominent features of Zn and Ge spectra are three close-lying $J^\pi=8^+$ that are qualitatively explained by an 8^+ of the ground-state band and the alignment of a proton and a neutron $g_{9/2}$ pair, several negative-parity bands, and a γ band. A recent semiphenomenological model[12] gives a quantitative explanation of these characteristics in ^{64,66}Zn and ^{66,68,70}Ge.

In this model a pair of quasiparticles of angular momentum J is coupled to an asymmetric triaxial rotor core of angular momentum R to form a state of total angular momentum I. For the positive-parity states both particles are in the $g_{9/2}$ single-particle orbital, and for the negative-parity states one nucleon is in $g_{9/2}$, while the other is in a $2p_{3/2}$, $2p_{1/2}$, or $1f_{5/2}$ orbital. Amplitude mixing in the wave functions is explicitly given for ^{68}Ge and ^{66}Ge. The lowest 8^+ state characterized by R $(=I)$ only, corresponds to the ground-state rotational band (97.2% of the wave function for ^{68}Ge). The second 8^+ state contains an aligned neutron pair $\nu_1^2=(\nu g_{9/2})^2_{J^\pi=8^+}$ and rotations from the core with a kinematical moment

TABLE III. Excitation energy, spin, and parity of ^{64}Zn levels.

Previous works			Present work					
E_x (MeV)	J^π	Band[c]	E_x (MeV)	$d\sigma/d\omega$[d] (μb/sr)	Configuration	CSM (MeV)	J^{π}[e]	
0.000[a,b]	0^+	g.s.	0.00					
0.991[a,b]	2^+	g.s.	0.98	76				
1.799[a,b]	2^+		1.80					
2.307[a,b]	4^+	g.s.	2.40					
2.998[a,b]	3^-	NP						
			3.06	434				
3.078[a,b]	4^+				$(\pi f_{5/2})^2_{4^+}$	3.514		
3.925[a,b]	5^-	NP						
3.993	6^+	g.s.						
4.156	5^-		4.10	530	$(\pi p_{3/2}\pi g_{9/2})_{5^-}$	4.096		
4.237	6^+							
4.635[a,b]	7^-	NP	4.65	185	$(\nu f_{5/2}g_{9/2})_{7^-}$	4.645		
4.981[a,b]	7^-							
5.151[a]	(6,7)							
			5.30	434	$(\pi f_{5/2}\pi g_{9/2})_{7^-}$	5.058	7^-	S,T
5.680[a,c]	$8^{(-)},(9)^-$	NP	5.70	186			(8^+)	S
6.124[a]	(9^-)				$(\nu g_{9/2})^2_{8^+}$	6.156		
			6.30					
6.766[a]			6.70	315	$(\pi g_{9/2})^2_{8^+}$	6.602	(8^+)	T
			7.40					
			7.90	521	$(\pi g_{9/2}\pi d_{5/2})_{6^+}$	7.572	(6^+)	T[f]

[a]Reference 22.
[b]Reference 20.
[c]Reference 23.
[d]Cross section at $\theta_{\text{lab}}=10°$ with an absolute error of 30%.
[e]Spin and parity assignments at the right in the table are based on systematic trends S and on crude shell-model (CSM) calculations (T).
[f]The 7.90-MeV peak is chosen as (6^+) rather than the 7.40-MeV one on yield considerations.

TABLE IV. Excitation energy, spin, and parity of ^{62}Zn levels.

Previous works			Present work					
E_x (MeV)	J^π	Band[e]	E_x (MeV)	$d\sigma/d\omega$[f] (μb/sr)	Configuration	CSM (MeV)	J^{π}[g]	
0.00[a,b]	0^+	g.s.	0.0					
0.95[a,b]	2^+	g.s.	0.96	19				
1.81[a,b]	2^+		1.80					
2.19[a,b]	4^+	g.s.	2.20					
3.20[b,c,e]	(3^-)	NP					3^-	S
			3.31	116				
3.216[d]	(4^+)				$(\pi f_{5/2})_{4^+}$	3.610	4^+	S,T
3.71[e]	6^+	g.s.						
4.05[b,e]	5^-	NP	4.17	141	$(\pi p_{3/2}\pi g_{9/2})_{5^-}$	4.391		
4.347[e]	6^+							
4.54[b]	6^+		4.50	47				
			4.70		$(\nu f_{5/2}\nu g_{9/2})^{7^-}$	4.795	7^-	S
4.90[a,e]	(7^-)							
5.122[e]	5,7	NP	5.19	171	$(\pi f_{5/2}\pi g_{9/2})_{7^-}$	5.361	7^-	T
			6.30		$(\nu g_{9/2})^2_{8^+}$	(6.673)	(8^+)	S
			7.54	106	$(\pi g_{9/2})^2_{8^+}$	7.112	(8^+)	T
			8.30	30	$(\pi g_{92}/\pi d_{5/2})_{6^+}$	(7.80)	(6^+)	T

[a]Reference 24.
[b]Reference 25.
[c]Reference 26.
[d]Reference 27.
[e]Reference 28.
[f]Cross section at $\theta_{lab}=10°$ with an absolute error of 30%.
[g]Spin and parity assignments at the right in the table are based on systematic trends S and on crude shell-model (CSM) calculations T.

TABLE V. Excitation energy, spin, and parity of ^{60}Zn levels.

Previous works			Present work					
E_x (MeV)	J^π	Band[d]	E_x (MeV)	$d\sigma/d\omega$[e] (μb/sr)	Configuration	CSM (MeV)	J^{π}[f]	
0.000[a]	0^+							
1.004[a]	2^+	g.s.	1.01	3				
2.193[a]	4^+	g.s.	2.19	3				
3.504[a]	3^-	NP	3.59	10				
			3.71		$(\pi f_{5/2})^2_{4^+}$	3.531		
3.82[b,d]	(0–4)		3.84					
4.200[d]		g.s.					(6^+)	S
4.36[a,b,d]	(2–6)		4.40	30	$(\pi p_{3/2}\pi g_{9/2})_{5^-}$	4.746	(5^-)	T
5.35[a,b]	4^+		5.30	27	$(\nu f_{5/2}\nu g_{9/2})_{7^-}$	(5.45)	(7^-)	S,T
					$(\pi f_{5/2}\pi g_{9/2})_{7^-}$	5.660		
6.63[a,c,d]	(0–4)							
			6.95	16	$(\nu g_{9/2})^2_{8^+}$	(7.24)	(8^+)	S
7.38[a,c]			7.35					
7.66[a,b]								
			7.98	8	$(\pi g_{9/2})^2_{8^+}$	7.788	(8^+)	T
			8.30	6	$(\pi g_{9/2}\pi d_{5/2})_{6^+}$	8.326	(6^+)	T
8.73[a,c,]			8.75		$(\pi d_{5/2})^2_{4^+}$	8.863	(4^+)	T

[a]Reference 29.
[b]Reference 30.
[c]Reference 31.
[d]Reference 32.
[e]Cross section at $\theta_{lab}=10°$ with an absolute error of 30%.
[f]Spin and parity assignments at the right in the table are based on systematical trends S and on crude shell-model (CSM) calculations T.

TABLE VI. Excitation energy, spin, and parity of ^{76}Ge levels.

Previous works			Present work					
E_x (MeV)	J^π	Band[c]	E_x (MeV)	$d\sigma/d\omega$[d] (μb/sr)	Configuration	CSM (MeV)	J^{π}[e]	
0.000[a]	0^+	g.s.	0.0					
1.039[a]	2^+	g.s.	1.03	72				
2.153[a]	4^+	g.s.	2.13					
2.561[a]	3^-	NP	2.55	173				
3.059[a]	4^+		3.05	317	$(\pi f_{5/2})^2_{4^+}$	3.071		
3.297[a]	6^+	g.s.						
			3.50	101				
3.417[a]	5^-	NP						
3.568[a]	$(2^- - 6^-)$				$(\pi p_{3/2}\pi g_{9/2})_{5^-}$	3.893		
3.955[a]	7^-	NP	4.02	220	$(\nu f_{5/2}\nu g_{9/2})_{7^-}$	3.744		
4.202[a]	8^+	g.s.			$(\nu g_{9/2})^2_{8^+}$	(4.142)		
			4.33	591				
4.30[b]	(7^-)				$(\pi f_{5/2}\pi g_{9/2})_{7^-}$	4.467	7^-	T,S
4.430[a]	8^+							
4.984[a]			4.92					
			5.42					
			5.73		$(\pi g_{9/2})^2_{8^+}$	5.863	(8^+)	T
			6.60		$(\pi g_{9/2}\pi d_{5/2})_{6^+}$	(6.377)	(6^+)	T
			7.04		$(\pi d_{5/2})^2_{4^+}$	(6.891)	(4^+)	T

[a]Reference 33.
[b]Reference 34.
[c]Reference 35.
[d]Cross section at $\theta_{lab}=10°$ with an absolute error of 30%.
[e]Spin and parity assignments at the right in the table are based on systematic trends S and on crude shell-model (CSM) calculations T.

TABLE VII. Excitation energy, spin, and parity of ^{68}Ge levels.

Previous works			Present work					
E_x (MeV)	J^π	Band[d]	E_x (MeV)	$d\sigma/d\omega$[e] (μb/sr)	Configuration	CSM (MeV)	J^{π}[f]	
0.000[a,b]	0^+	g.s.	0.0					
1.016[a,b,c]	2^+	g.s.	1.03	22				
1.778[a,b,c]	2^+		1.80					
2.268[a,b,c]	4^+	g.s.	2.28					
2.649[a,b]	3^-	NP	2.66	148				
3.041[a]	(4^+)		3.05	116	$(\pi f_{5/2})^2_{4^+}$	2.838	4^+	S,T
3.650[c]	5^-	NP	3.67	130	$(\pi p_{3/2}\pi g_{9/2})_{5^-}$	4.194		
3.696[a,c]	6^+	g.s.						
4.054[c]	7^-	NP	4.08	292	$(\nu f_{5/2}\nu g_{9/2})_{7^-}$	(4.056)		
			4.61	156	$(\pi f_{5/2}\pi g_{9/2})_{7^-}$	4.553	7^-	T
4.837[a,c]	(8^+)	g.s.	4.81	210	$(\nu g_{9/2})^2_{8^+}$	(4.790)	8^+	S
5.151[a]			5.18					
			5.56					
			6.30		$(\pi g_{9/2})^2_{8^+}$	6.268	(8^+)	T
			6.96		$(\pi g_{9/2}\pi d_{5/2})_{6^+}$	(6.940)	(6^+)	T

[a]Reference 36.
[b]Reference 37.
[c]Reference 38.
[d]Reference 39.
[e]Cross section at $\theta_{lab}=10°$ with an absolute error of 30%.
[f]Spin and parity assignments at the right in the table are based on systematic trends S and on crude shell-model (CSM) calculations T.

TABLE VIII. Excitation energy, spin, and parity of ^{66}Ge levels.

Previous works			Present work					
E_x (MeV)	J^π	Band[c]	E_x (MeV)	$d\sigma/d\omega$[d] (μb/sr)	Configuration	CSM (MeV)	J^{π}[e]	
0.000[a,b]	0^+	g.s.	0.0					
0.957[a,b]	2^+	g.s.	0.93	1				
2.174[a,b]	4^+	g.s.	2.17					
2.799[a,c]	(3^-)	NP	2.80	37			3^-	S
3.025[a,c]	$(3^-,5^-)$							
3.080[a]			3.06	11	$(\pi f_{5/2})_{4^+}$	2.699	4^+	S,T
3.656[a,b,c]	(6^+)	g.s.	3.60					
3.685[a,b,c]	5^-	NP						
3.830[a,b,c,]	$(3^-,5^-)$		3.83	94	$(\pi p_{3/2}\pi g_{9/2})_{5^-}$	4.357	5^-	S,T
3.841[a]								
4.207[a,b,c]	7^-	NP	4.20	83	$(\nu f_{5/2}\nu g_{9/2})_{7^-}$	4.557		
4.544[a,b,c]			4.59	53	$(\pi f_{5/2}\pi g_{9/2})_{7^-}$	4.548	(7^-)	S,T
			4.92	45				
5.495[a,b,c]	$(6\text{–}9)^-$	NP						
			5.50	37	$(\nu g_{9/2})^2_{8^+}$	5.662	8^+	S
5.534[a]	(8^+)							
6.505[a]								
			6.63	71	$(\pi g_{9/2})^2_{8^+}$	6.397	(8^+)	T
			7.27	76	$(\pi g_{9/2}\pi d_{5/2})_{6^+}$	(7.179)	(6^+)	T

[a]Reference 19.
[b]Reference 40.
[c]Reference 41.
[d]Cross section at $\theta_{\text{lab}}=10°$ with an absolute error of 30%.
[e]Spin and parity assignments at the right in the table are based on systematic trends S and on crude shell-model (CSM) calculations T.

TABLE IX. Single-particle energies (MeV) used in the crude shell-model calculations.

	$2p_{3/2}$	$1f_{5/2}$	$2p_{1/2}$	$1g_{9/2}$	$2d_{5/2}$
^{59}Cu[a]	0	0.914	0.491	3.043	3.580
^{61}Cu[b]	0	0.970	0.475	2.721	(3.406)
^{63}Cu[c]	0	0.962	0.670	2.506	3.476
^{65}Cu[d]	0	1.115	0.771	2.534	(3.391)
^{65}Ga[d]	0	0.191	(0.062)	2.040	(2.822)
^{67}Ga[e]	0	0.359	0.167	2.074	(2.746)
^{69}Ga[f]	0	0.574	0.319	1.970	(2.484)
^{59}Ni[a]	0	0.339	0.465	3.055	4.462
^{61}Ni[b]	0	0.067	0.283	2.122	2.697
^{63}Ni[c]	0.155	0.087	0	(1.292)	2.297
^{65}Ni[d]	0.692	0	0.063	1.013	1.920
^{59}Zn[a,g]	0	(0.90)	(0.54)	(2.68)	
^{61}Zn[b]	0	0.124	(0.088)	(2.002)	
^{63}Zn[c]	0	0.193	0.248	1.704	
^{65}Zn[d]	0.115	0	(0.054)	1.065	1.370
^{65}Ge[h]	0	0.111		1.216	
^{67}Ge[e]	(0.123)	(0.018)	(0)	(0.752)	
^{69}Ge[f]	0.233	0	0.087	(0.398)	

[a]Reference 42.
[b]Reference 43.
[c]Reference 44.
[d]Reference 45.
[e]Reference 46.
[f]Reference 47.
[g]Reference 50.
[h]Reference 51.

$R=0$ and $R=2$ (64 and 20%, respectively of the wave functions for ^{68}Ge). The third band (ν_2^2) corresponds to two $g_{9/2}$ neutrons coupled to 6^+ with the core. Petrovici and Faessler[12] predict an 8^+ state formed by two aligned protons $(\pi g_{9/2})^2_{J^\pi=8^+}$ at higher energies, or for ^{68}Ge about 1 MeV higher than the third 8^+ state.

While the 3^- level is almost an equal admixture of $(\pi p_{3/2}\pi g_{9/2})_{3^-}$ $R=0$ and $(\nu p_{3/2}\nu g_{9/2})_{3^-}$ $R=0$ configurations, two favored negative-parity bands NP1 and NP2 with total angular momentum $I=J+R$ are at higher spins characterized by $(\nu g_{9/2}\nu f_{5/2})_{J=7}$ and $(\pi g_{9/2}\pi f_{5/2})_{J=7}$. NP3 is an unfavored negative-parity band characterized with $I=R+J-1$ and $(\nu g_{9/2}\nu f_{5/2})_{J=7}$ at higher spins.

IV. RESULTS

The measured spectra are presented in Figs. 3–7. In Tables II–VII the experimental excitation energies, given with a precision of 50 keV, are compared with previously known levels for ^{66,64,62,60}Zn and ^{70,68,66}Ge nuclei, and absolute differential cross sections are reported. These latter have been determined to about 30% and, depending on the transition and on the target for the well-fed transitions, range from 20–500 μb/sr for $2p$ transfer on Ni isotopes (Fig. 5), 100–600 μb/sr for $2p$ transfer on Zn isotopes (Fig. 6), and 60–300 μb/sr for $2n$ transfer on Ni isotopes (Fig. 7). The $2n$ values have to be compared with (α,^{2}He) cross sections, namely about 50 μb/sr for transitions to the preferentially populated final states.[6] Angular distributions in 1° slices have been obtained over the 6° aperture of the spectrometer and fitted with exact finite range (EFR) DWBA calculations (code PTOLEMY) and parameters taken from Ref. 18. Figure 8 shows the fit to the partial angular distribution of a 3^- level in ^{66}Zn and a 7^- level in ^{68}Ge. Though the shapes of the angular distributions are not typical enough to serve as a J^π signature, it is possible to distinguish from the slope between large and low spin values. Values of the deduced relative spectroscopic factor α are effectively found close to 1 for high-spin states expected as $2N$ levels, but a more refined analysis taking account of multistep processes would be more adequate.

The ^{66}Zn spectrum obtained by $2p$ transfer (Fig. 3) differs from that of the $2n$ transfer spectrum (Fig. 4) in that it shows a larger number of peaks superimposed on a more important background.

The selectivity of the $2n$ reaction is well explained by the predominant excitation of the configurations $(\nu f_{5/2}\nu g_{9/2})_{7^-}$, $(\nu g_{9/2})^2_{8^+}$, and $(\nu g_{9/2}\nu 2d_{5/2})_{6^+}$ as shown by Jahn[6] with the (α,^{2}He) reaction. The yet not reported peak at 6.25 MeV could correspond to the $(\nu 2d_{5/2})^2_{4^+}$ configuration calculated with the CSM to lie at 5.819 MeV. The same predominance of the $(\pi f_{5/2}\pi_{9/2})_{7^-}$, $(\pi g_{9/2})^2_{8^+}$, and $(\pi g_{9/2}\pi 2d_{5/2})_{6^+}$ stretched natural-parity configurations, predicted at 5.119, 6.535, and 7.374 MeV, respectively, was expected for the $2p$ spectrum.[10] While the peaks at 5.20, 6.85, and 7.55 MeV are good candidates for these states, there are several other strong peaks, some corresponding to known states.[19] Indeed, in the $2p$ transfer case the $2p_{3/2}$, $2p_{1/2}$, and $f_{5/2}$ shells are all available. The filling of these shells leads to configurations of final spin 3^-, 4^+, 5^-, and could explain the fact that the peaks from the 3^-, 4^+, and 5^- levels at 2.84, 3.06, and 3.74 MeV, respectively, are strongly excited in the ^{64}Ni(^{12}C,^{10}Be)^{66}Zn reaction, but not, or weakly, in ^{64}Zn(^{12}C,^{10}C)^{66}Zn. In particular, the 5^- state (seen in γ-ray spectroscopy) probably has large $(\pi p_{3/2}\pi g_{9/2})_{5^-}$ and/or $(\pi p_{1/2}\pi g_{9/2})_{5^-}$ components. Two peaks corresponding to energies close to those of $2n$ states, i.e., the 4.20-MeV 7^- yrast state and the 5.25-MeV state, previously ascribed $(\nu f_{5/2}\nu g_{9/2})_{7^-}$ and $(\nu g_{9/2})^2_{8^+}$, are surprisingly also well excited in the $2p$ transfer. This argues for $2p$ components in these states also.

The same considerations hold for the ^{60,62,64}Zn (Fig. 5) and the ^{66,68,70}Ge spectra (Fig. 6) which appear less selective as the number of neutrons increases. This is contrary to what is observed in the $2n$ transfer spectra on ^{60,62,64,66}Ni (Fig. 7).

The greater neutron number (2–10) outside the closed $1f_{7/2}$ shell probably contributes to the loss of selectivity of the $2p$ transfer reactions on the even Ni and Zn iso-

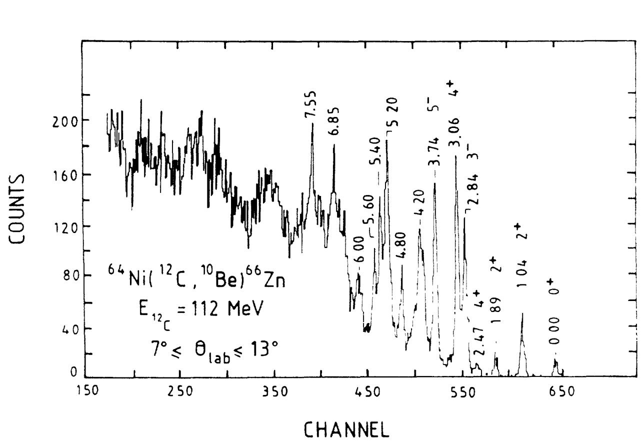

FIG. 3. The ^{66}Zn spectrum obtained by a $2p$ transfer reaction ($Q=-10.806$ MeV). This is to be compared with the ^{66}Zn spectrum of Fig. 4 obtained in the same conditions by a $2n$ transfer reaction ($Q=-12.083$ MeV).

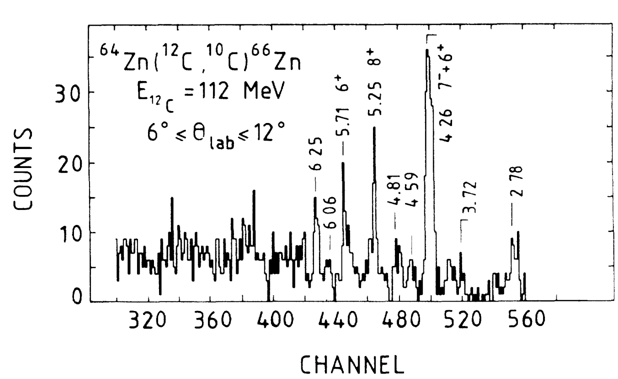

FIG. 4. See caption of Fig. 3.

topes, while the reduced proton number (0–2) outside the closed $1f_{7/2}$ shell is of no consequence for the same targets in the $2n$ transfer spectra (Fig. 7) in which the $(\nu 2p_{1/2}\nu g_{9/2})_{5^-}$, $(\nu f_{5/2}\nu g_{9/2})_{7^-}$, $(\nu f_{5/2}\nu 2d_{5/2})_{5^-}$, $(\nu g_{9/2})^2_{8^+}$, and $(\nu g_{9/2}\nu 2d_{5/2})_{6^+}$ configurations dominate.[6]

The background, which increases with the Q value of the reaction is more important in the $2p$ transfer spectra [$Q(2p) = -27.19$ MeV compared with $Q(2n) = -31.84$ MeV] and adds to the difficulty of their interpretation.

In Tables II–VIII are reported the J^{π} proposed on the basis of previous data, angular distribution analysis, systematic spectral trends S among even isotopes, and shell-model calculations of two-particle configurations (CSM). States related by $E2$ transitions in the referenced γ-ray

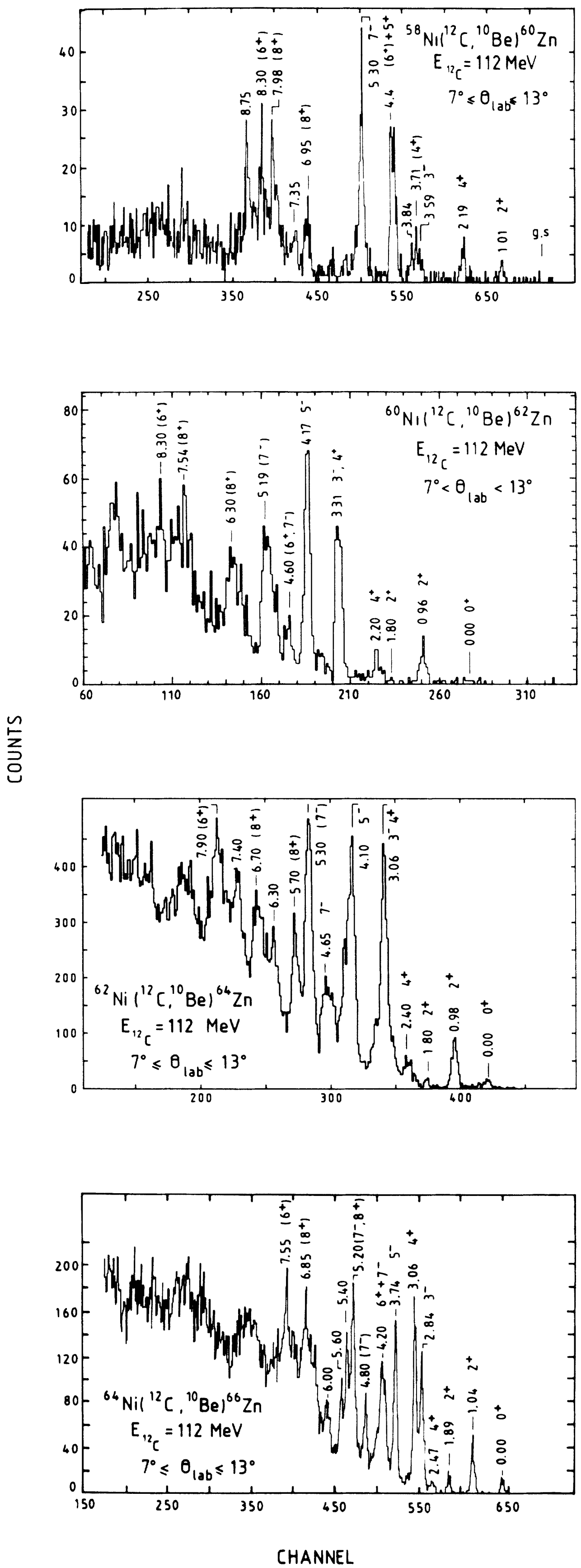

FIG. 5. Two-proton transfers on ^{58,60,62,64}Ni. The respective Q values are −18.647, −15.908, −13.350, and −10.806 MeV.

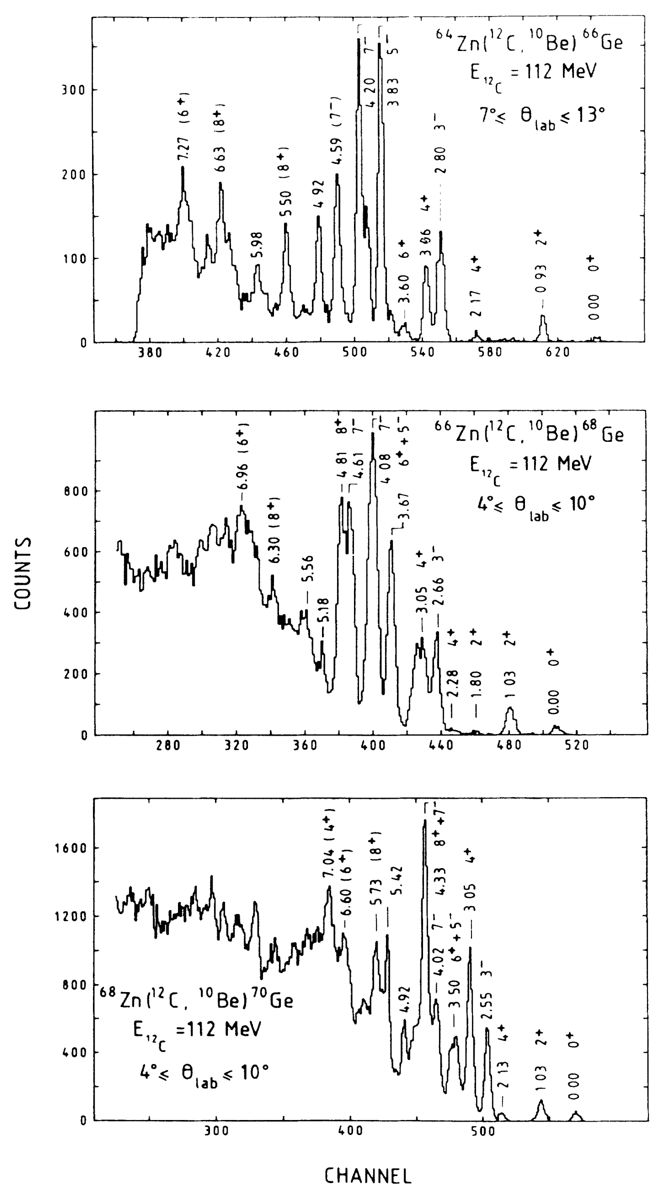

FIG. 6. Two-proton transfers on ^{64,66,68}Zn. The respective Q values are −16.989, −14.538, and −12.052 MeV.

scheme are indicated in the tables by g.s. and NP for ground-state positive, and negative-parity bands, respectively.

V. DISCUSSION

Two-proton aspects are dominant in the measured (^{12}C,^{10}Be) reaction spectra and the configurations $(\pi g_{9/2})^2_{8^+}$, $(\pi g_{9/2}\pi f_{5/2})_{7^-}$, $(\pi g_{9/2}\pi d_{5/2})_{6^+}$, and $(\pi g_{9/2}\pi p_{3/2})_{5^-}$ allow us to explain the observation of most of the strongest peaks. Table X shows the agreement between experimental and CSM calculated excitation energies. In Table XI are reported the TBME values deduced from the present work.

In Fig. 9 are drawn for each of the main configurations the experimental $2p$-binding energies versus the mass

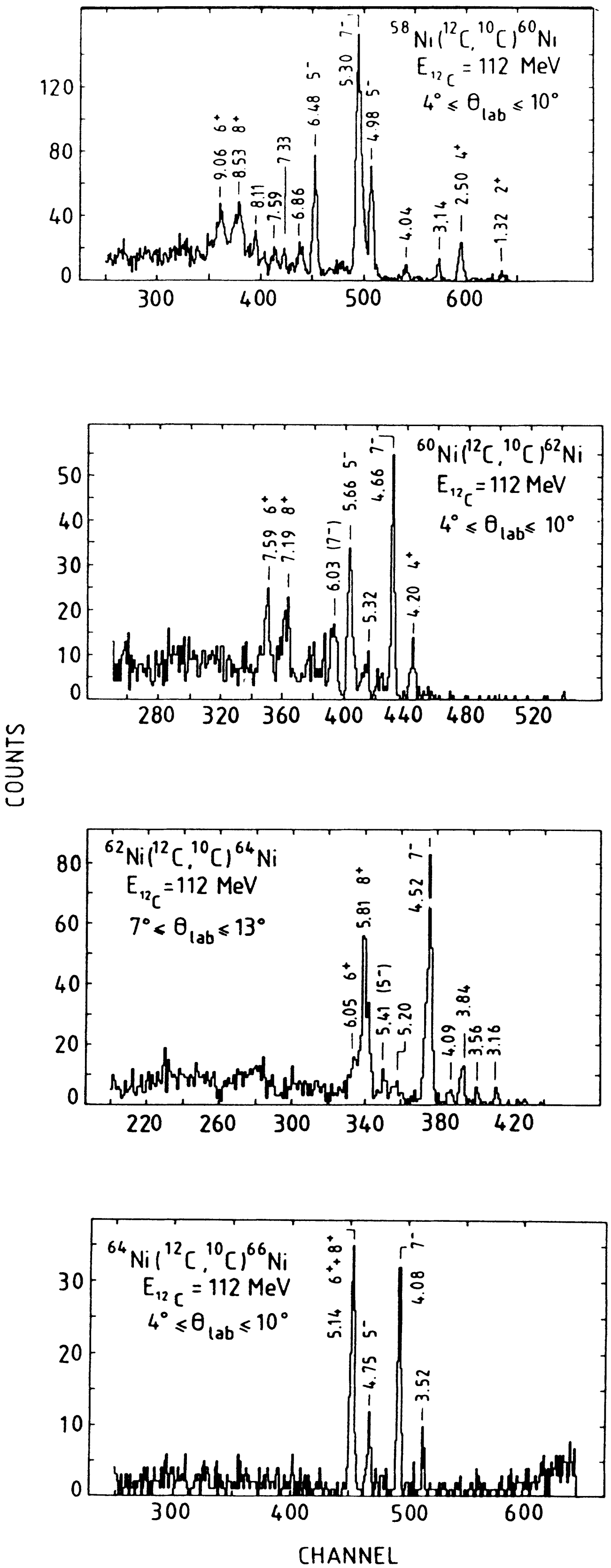

FIG. 7. Two-neutron transfers on ^{58,60,62,64}Ni. The respective Q values are −11.453, −13.424, −15.347, and −16.768 MeV. The J^π values are those deduced from the (α,^{2}He) reactions (Ref. 6).

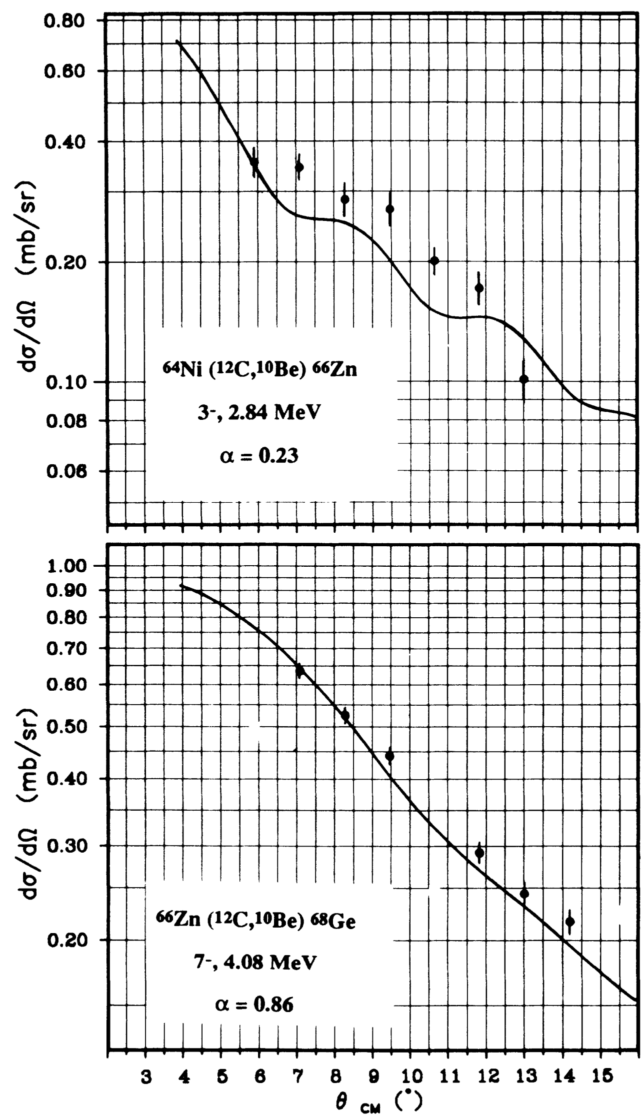

FIG. 8. Angular distributions over the 6° aperture of the spectrometer The continuous line is a DWBA fit with the parameters of Ref. 18.

TABLE X. Crude shell model and experimental energies (MeV) of assumed $2p$ states in Zn and Ge isotopes.

	$(\pi f_{5/2} \pi g_{9/2})_{7^-}$		$(\pi g_{9/2})^2_{8^+}$		$(\pi g_{9/2} \pi d_{5/2})_{6^+}$		$(d_{5/2})^2_{4^+}$	
^{60}Zn	5.660	5.30	7.788	7.98	8.326	8.30	8.863	8.75
^{62}Zn	5.361	5.19	7.112	7.54	(7.80)	7.54	(8.482)	
^{64}Zn	5.058	5.30	6.602	6.70	7.572	7.90	8.542	
^{66}Zn	5.122	5.20	6.541	6.85	(7.398)	7.55	(8.255)	
^{66}Ge	4.548	4.59	6.397	6.63	7.179	7.27	(7.961)	
^{68}Ge	4.553	4.61	6.268	6.30	6.940	6.96	(7.612)	
^{70}Ge	4.467	4.33	5.863	5.73	(6.377)	6.60	(6.891)	

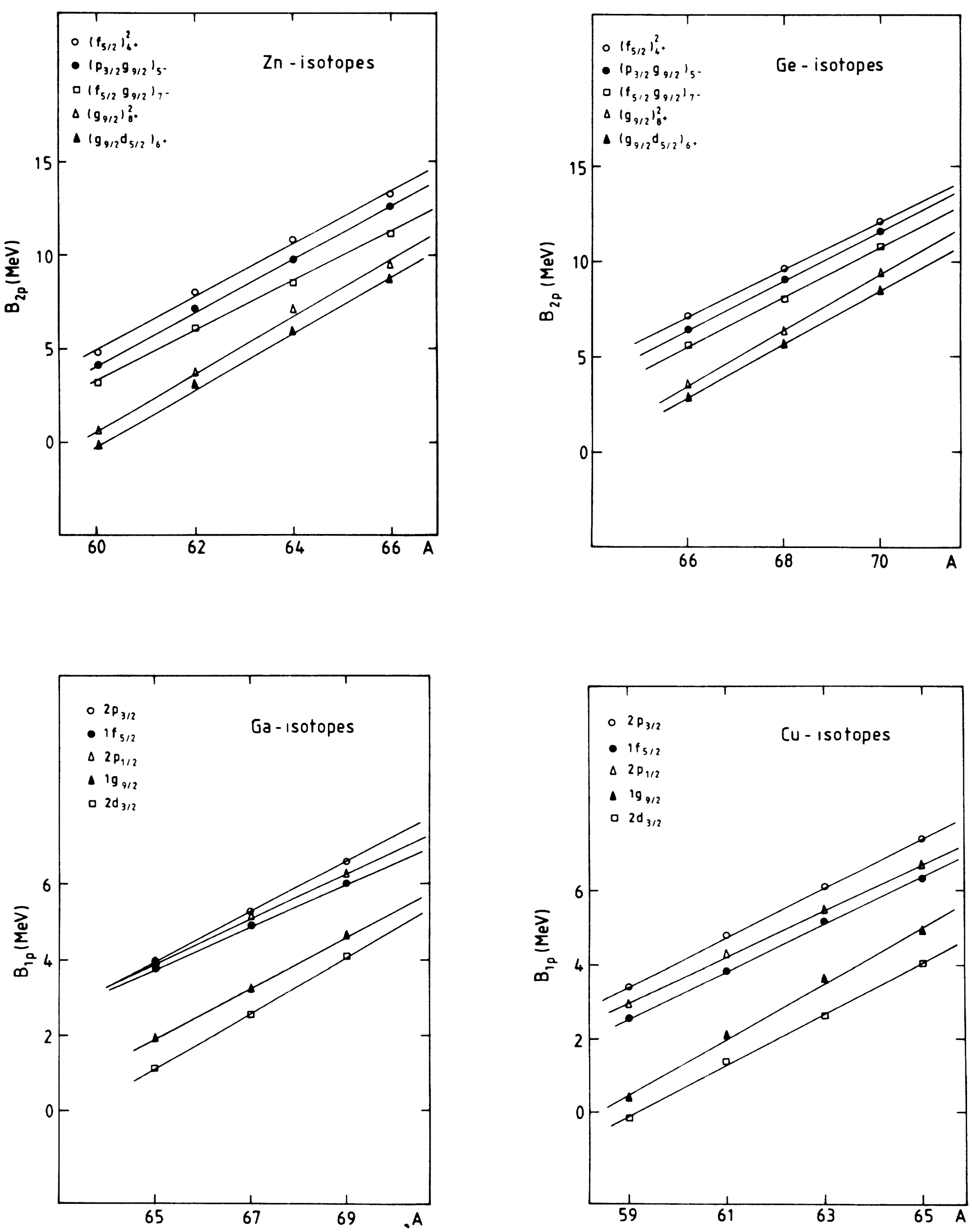

FIG. 9. Two-proton binding energies deduced from the present work for Zn and Ge even isotopes and reported one-proton binding energies for $^{59-65}$Cu and $^{65-69}$Ga odd isotopes. The coefficients of the least-square linear fits are reported in Table XII.

TABLE XI. Two-body matrix elements for Zn and Ge isotopes (MeV).

Configuration	Previous values	Present work[a] ^{60}Zn	^{62}Zn	^{64}Zn	^{66}Zn	^{66}Ge	^{68}Ge	^{70}Ge	Mean values
$(f_{5/2})^2_{4^+,1}$	+0.461[17]	+0.18	−0.30	−0.45	−0.64	+0.36	+0.21	−0.02	−0.09±0.35
$(p_{3/2}g_{9/2})_{5^-,1}$		−0.35	−0.22	+0.00	−0.27	−0.53	−0.52	−0.39	−0.33±0.18
$(f_{5/2}g_{9/2})_{7^-,1}$	−0.10±0.35[6]	−0.36	−0.17	+0.24	−0.32	+0.04	+0.06	−0.14	−0.09±0.22
$(g_{9/2})^2_{8^+,1}$	+0.22±0.51[6]	+0.19	+0.43	+0.10	+0.31	+0.23	+0.03	−0.13	+0.17±0.17
$(g_{9/2}d_{5/2})_{6^+,1}$	+0.18±0.63[6]	−0.03	+0.50	+0.33	+0.15	+0.09	+0.02	+0.22	+0.18±0.17

[a]These two-proton configuration values include the Coulomb interaction energy.

number A of the final nucleus

$$B_{2p}(A_0+2,J)=E_B(A_0+2,\text{g.s.})-E_B(A_0,\text{g.s.})+E^*(A_0+2,J)\ .$$

These binding energies vary linearly with A, as observed[6] for the $2n$ states fed by the $(\alpha,{}^2\text{He})$ reaction on the $1f$-$2p$ shell nuclei and as predicted by the Bansal-French model.[11]

In this model, the $2p$-binding energy of a level in a nucleus of mass A and atomic number Z is written

$$B_{2p}(A,JT)=B_{2p}(A_0+2,JT_0)-2a(A_0+2-A)+b(T-1)+c(A_0+2-A+2T_Z) \qquad (5)$$

with the isospin $T=T_Z=(A/2)-Z$ for the considered nuclei. Then,

$$B_{2p}(A,JT)=\left[2a+\frac{b}{2}\right]A+B_{2p}(A_0+2,JT_0)-2a(A_0+2)-b(Z+1)+c(A_0+2-2Z)\ .$$

For isotopes of an element Eq. (5) depends on A only:

$$B_{2p}=kA+l\ .$$

This linear dependence results from the linear dependence of the $1p$-binding energies versus A. In effect

$$B_{1p}(A,JT)=B_{1p}(A_0+1,JT_0)-a(A_0+1-A)+\frac{b}{2}(T-\tfrac{1}{2})+\frac{c}{2}(A_0+1-A+2T_z)\ ,$$

which can be written

$$B_{1p}(A,JT)=\left[a+\frac{b}{4}\right]A+B_{1p}(A_0+1,JT_0)-a(A_0+1)-\frac{b}{2}(Z+\tfrac{1}{2})+\frac{c}{2}(A_0+1-2Z)\ .$$

For isotopes of an element

$$B_{1p}(A,JT)=k'A+l'$$

with

$$k'=a+\frac{b}{4}=\frac{k}{2}\ ,$$

$$l'=B_{1p}(A_0,JT_0)-a(A_0+1)-\frac{b}{2}(Z+\tfrac{1}{2})+\frac{c}{2}(A_0+1-2Z)\ .$$

The coefficients k, l, k', and l' are determined from a least-square fit of the experimental binding-energy values (Fig. 9) and reported in Table XII. The values of k,l are clearly correlated to k',l' and we have $k=k'_1+k'_2$, $l=l'_1+l'_2$ to less than 10%. The linearity observed in the $2p$ case reflects the linearity in the $1p$ case.[10]

In each of the Tables II–VIII appears one positive-parity g.s. and one negative-parity (NP) band which could be associated with the ground-state rotational (GSRB) and one of the negative-parity bands of Petrovici and Faessler.[12]

The ground-state band previously known up to 6^+ in ^{62,64,66}Zn and ^{66,68,70}Ge is excited weakly in the corre-

TABLE XII. Coefficients k, l, k' and l' deduced from the linear least-square fits of the experimental two-proton and one-proton binding-energy values.

		$(f_{5/2})^2_{4^+}$	$(p_{3/2},g_{9/2})_{5^-}$	$(f_{5/2},g_{9/2})_{7^-}$	$(g_{9/2})^2_{8^+}$	$(g_{9/2}d_{5/2})_{6^+}$
Zn	k	1.413	1.406	1.313	1.515	1.515
	l	−79.895	−80.207	−75.493	−90.239	−91.151
Ge	k	1.235	1.315	1.208	1.458	1.400
	l	−74.425	−80.479	−80.132	−92.722	−89.535
		$2p_{3/2}$	$1f_{5/2}$	$2p_{1/2}$	$1g_{9/2}$	$2d_{5/2}$
Cu	k'	0.671	0.641	0.619	0.758	0.696
	l'	−36.180	−35.326	−33.575	−44.282	−41.184
Ga	k'	0.665	0.570	0.601	0.683	0.750
	l'	−39.341	−33.301	−35.219	−42.542	−47.687

sponding spectra. In ^{60}Zn the γ-ray scheme is not well known.[29] A recent (^{3}He,$n\gamma$) study[32] performed at a 12-MeV incident energy leads to low J^{π} value levels, weakly or not fed in our spectrum. The probable doublet peak we observe at 4.40 MeV could contain the 6^+ ground-state band member, if it follows the trend in the location of the 6^+ states in the other nuclei.

Of the three 8^+ branches in forks reported in some of the Zn and Ge isotopes there subsists only one 8^+ state in our spectra, very close to the calculated position of the $(\nu g_{9/2})^2_{8^+}$ configuration. In ^{68}Ge where the triple forking was first observed,[48] the nature of the 8^+ states at 4.837, 5.050, and 5.367 MeV differs according to several interpretations.[12,38,49] Recent g-factor measurements[39] order them as ν_1^2, ν_2^2, and GSRB states. This does not agree with the order calculated by Petrovici and Faessler[12] and lends support to the importance of the neutrons of the target outside the closed $f_{7/2}$ shell, as mentioned in Sec. IV. This leads us to propose that the peaks at 5.50 MeV in ^{66}Ge and 5.20 MeV in ^{66}Zn are 8^+ levels of the same $(\nu_{9/2})^2$ configuration. The same assumption for peaks at 5.70 MeV in ^{64}Zn and 6.30 MeV in ^{62}Zn is more questionable because the correspondence with the calculated energy is not as good and the collectivity effect is expected to decrease with the neutron number.

Calculation of the energy of the $(\nu g_{9/2})^2_{8^+}$ configuration in ^{60}Zn requires the position of the $g_{9/2}$ single-particle state in ^{59}Zn that is yet unknown.[42] A level seen at 2.68 MeV in the ^{58}Ni$(p,\pi^-)^{59}$Zn reaction[50] is a possible candidate and would lead to a $(\nu g_{9/2})^2_{8^+}$ excitation energy of 7.24 MeV, which is close to the 6.95-MeV peak in ^{60}Zn that systematics indicates as an 8^+ state.

Three strong peaks observed in the ^{66}Zn and ^{70,68}Ge spectra belong to a known negative-parity band (see Tables II, VI, and VII). Respectively, the 3^- members are at 2.84, 2.66, and 2.55 MeV, while the 5^- members are at 3.74, 3.67, and 3.50 MeV (not resolved in our spectra from the 6^+ GSRB member in the two last cases) and the 7^- members are at 4.20 MeV (also mixed with the 6^+ GSRB member), 4.08 and 4.02 MeV. In the isotones ^{64}Zn and ^{66}Ge (see Tables III and VIII) the 3^-, 5^-, 7^- members of the same band are reported at 2.998, 3.925, and 4.635 MeV and at (2.799), 3.685, and 4.207 MeV, respectively. All of these states correspond to intense peaks in our spectra except the 5^- members that are weakly excited. The agreement between the location of the 7^- members, and the calculated energy of the $(\nu f_{5/2}\nu g_{9/2})_{7^-}$ configuration as well as the apparent dependence of the relative yields on the neutron number of the target nuclei lead us to propose that we excite the negative-parity band NP1 of Petrovici and Faessler[12] that is composed of mixed neutron and proton configurations for lower spins, and levels of mainly $(\nu f_{5/2}\nu g_{9/2})_{J=7}$ $I=J+R$ nature for higher spins.

A second negative-parity band NP2 built on a 5^- state is predicted[12] a little higher in energy with a main configuration $(\pi f_{5/2}\pi g_{9/2})_{J=7}$ $I=J+R$. In fact, the calculated energies of the high-spin stretched $2p$ states, which are expected to be strongly excited, correspond to those of the remaining strong spectral peaks. However, few of these states were previously J^{π} assigned or even known (see Tables II–VIII). We propose 4^+ as J^{π} for the 3.71- or 3.82-MeV state in ^{60}Zn and the 3.06-MeV state in ^{66}Ge, because these levels are close to the calculated energy of the $(\pi f_{5/2})^2_{4^+}$ configuration and also in agreement with the systematic trend. The $(\pi p_{3/2}\pi g_{9/2})_{5^-}$ configuration compatible with all of the previous assignments (see Tables II–VIII) is often close in energy to the 5^- member of the NP1 band, and in some cases, it is difficult to distinguish between them. In ^{64}Zn and ^{66,70}Ge, where the NP1 member corresponds to the lowest reported 5^- state, we attribute on yield arguments the $(\pi p_{3/2}\pi g_{9/2})_{5^-}$ configuration to the 4.156-, 3.830-(3^-,5^-), and 3.568-MeV (2^-–6^-) states, respectively. In ^{68}Ge two 5^- states are reported at 3.582 and 3.650 MeV, but are not distinguishable in our spectrum. Because of the systematic trends and the relative γ-ray decay rate[39] of the 4.054 MeV, 7^- NP1 member to the 3.582 MeV, 5^- state (52%) and the 3.650 MeV, 5^- state (31%), we argue that the 5^- NP1 member is at 3.582 MeV and that the 3.650 MeV, 5^- state, is mainly of a $(\pi p_{3/2}\pi g_{9/2})_{5^-}$ configuration. The same configuration could explain the important peaks at 4.40 MeV previously J assigned (2–6) in ^{60}Zn, at 4.17 MeV in ^{62}Zn and 3.74 MeV in ^{66}Zn.

For all the considered nuclei there exist peaks in the vicinity of the predicted values for the $(\pi f_{5/2}\pi g_{9/2})_{7^-}$, $(\pi g_{9/2})^2_{8^+}$, and $(\pi d_{5/2}\pi g_{9/2})_{6^+}$ configurations (see Tables II–VIII). Reported (7^-) states at 4.814 MeV in ^{66}Zn and 4.30 MeV in ^{70}Ge reinforce our proposition for the 4.80-MeV peak (Fig. 5) and the 4.33-MeV peak (Fig. 6).

VI. CONCLUSION

The present study of the (^{12}C,^{10}Be) $2p$ transfer reactions with 112-MeV ^{12}C on Ni and Zn isotopes reveals new $2p$ levels in the ^{60,62,64,66}Zn and ^{66,68,70}Ge final nuclei and leads to high-spin and parity assignments that are proposed on systematical trends, and crude shell-model calculations, and are supported by the Bansal-French model.[11]

This work complements the (α,^{2}He) $2n$ transfer reaction data.[6] The $(\pi g_{9/2})^2_{8^+}$ and $(\pi g_{9/2}\pi d_{5/2})_{6^+}$ states located a few MeV higher than the corresponding $2n$ states are not populated by fusion-evaporation reactions, but some proposed $(\pi f_{5/2}\pi g_{9/2})_{7^-}$ states could be identified with 7^- states seen in γ spectroscopy. The lesser selectivity of the $2p$ transfer as compared to the $2n$ transfer on the same targets can be related to the greater number of neutrons than protons outside the closed $f_{7/2}$ shell in the target. This fact adds some collectivity to the spectra that are well explained by the asymmetric rotor model with an admixture of two quasiparticles.[12] It explains why we can have serious doubts about whether DWBA calculations could be trusted for the two-proton transfer nuclei discussed here, but a more refined theoretical analysis taking into account multistep processes lies beyond the scope of this work.

Increasing the incident energy should enhance the selectivity as has been found for $2p$ transfers on ^{54}Fe and lighter targets with 40-MeV/nucleon ^{12}C projectiles,[7] and the evolution of the spectra with energy could be interesting to locate the two-proton stretched states.

ACKNOWLEDGMENTS

We thank R. Jahn for sending us a copy of his thesis, and J. A. Cameron for communicating data prior to publication on ^{60}Zn and ^{61}Zn contained in the thesis of R. B. Schubank. Useful discussions with N. Schulz and the critical comments of A. Pape on the manuscript are gratefully acknowledged. We are indebted to F. Jundt and J. C. Sens who participated in the early stages of this work. Thanks are due to the staffs of the MP accelerator and of the Q3D spectrometer for their important assistance. One of us (A.B.) acknowledges the guidance and help of R. Seltz and the financial support from the country of Algeria.

*On leave from the University of Setif, Algeria.

[1]*Table of Isotopes*, 7th ed., edited by C. M. Lederer and V. S. Shirley (Wiley, New York, 1978).

[2]C. C. Lu, M. S. Zisman, and B. G. Harvey, Phys. Rev. **186**, 1086 (1969).

[3]N. Anyas-Weiss, J. C. Cornell, P. S. Fisher, P. N. Hudson, A. Menchaca-Rocha, D. J. Millener, A. D. Panagiotou, D. K. Scott, D. Strottman, D. M. Brink, B. Buck, P. J. Ellis, and T. Engeland, Phys. Rep. **12C**, 201 (1974).

[4]R. Jahn, D. P. Stahel, G. J. Wozniak, R. J. de Meijer, and J. Cerny, Phys. Rev. C **18**, 9 (1978).

[5]R. Jahn, U. Wienands, D. Wenzel, and P. von Neumann-Cosel, Phys. Lett. **150B**, 331 (1985).

[6]R. Jahn, thesis, Institut für Strahlen und Kernphysik der Universität Bonn, 1985.

[7]L. Kraus, A. Boucenna, I. Linck, B. Lott, R. Rebmeister, N. Schulz, J. C. Sens, M. C. Mermaz, B. Berthier, R. Lucas, J. Gastebois, A. Gillibert, A. Miczaika, E. Tomasi-Gustafsson, and C. Grunberg, Phys. Rev. C **37**, 2529 (1988).

[8]Tsan Ung Chan, J. F. Bruandet, B. Chambon, A. Dauchy, D. Drain, A. Giorni, F. Glasser, and C. Morand, Nucl. Phys. **A348**, 179 (1980).

[9]Tsan Ung Chan, M. Agard, J. F. Bruandet, and C. Morand, Phys. Rev. C **19**, 244 (1979).

[10]Tsan Ung Chan, Phys. Rev. C **36**, 838 (1987).

[11]R. K. Bansal and J. B. French, Phys. Lett. **11**, 145 (1964).

[12]A. Petrovici and Amand Faessler, Nucl. Phys. **A395**, 44 (1983).

[13]D. M. Brink, Phys. Lett. **40B**, 37 (1972).

[14]M. Mermaz, Etude du Mécanisme des Réactions Induites par Ions Lourds de Masse Inférieure à Vingt, Commissariat à l'Energie Atomique, Departement de Physique Nucléaire, 1983, p. 131.

[15]P. J. Brussaard and P. W. M. Glaudemans, *Shell Model Applications in Nuclear Spectroscopy* (North-Holland, Amsterdam, 1977), p. 41.

[16]G. Audi and A. Wapstra, The 1986 Audi-Wapstra MID-Stream Mass Evaluations, distributed by P. Haustein, Brookhaven National Laboratory, Upton, New York, 1986.

[17]T. T. S. Kuo, Nucl. Phys. **A90**, 199 (1967).

[18]H. Homeyer, F. D. Bechetti, B. G. Harvey, D. L. Hendrie, D. G. Kovar, J. Mahoney, and W. von Oertzen, Lawrence Berkeley Laboratory Report No. LBL-4000, 1975, p. 67.

[19]N. J. Ward and F. Kearns, Nucl. Data Sheets **39**, 1 (1983).

[20]J. Jabbour, L. H. Rosier, B. Ramstein, R. Tamisier, and P. Avignon, Nucl. Phys. **A464**, 260 (1987).

[21]G. F. Neal, Z. P. Zawa, F. P. Venezia, and P. R. Chagnon, Nucl. Phys. **A280**, 161 (1977).

[22]H. L. Halbert, Nucl. Data Sheets **28**, 179 (1979).

[23]D. N. Simister, L. P. Ekström, G. D. Jones, F. Kearns, T. P. Morrison, O. M. Mustaffa, H. G. Price, P. J. Twin, R. Wadsworth, and N. J. Ward, J. Phys. G **6**, 81 (1980).

[24]H. L. Halbert, Nucl. Data Sheets **26**, 5 (1979).

[25]Y. Okuma, T. Yanabu, T. Motobayashi, K. Takimoto, S. Mitsuki, K. Ogino, T. Shimoura, M. Fukada, and T. Suehiro, Osaka Research Center for Nuclear Physics report, 1982, p. 92.

[26]G. P. A. Berg, B. Berthier, J. P. Fouan, J. Gastebois, J. P. Le Févre, and M. C. Lemaire, Phys. Rev. C **18**, 2204 (1978).

[27]H. Verheul, Nucl. Data Sheets **13**, 443 (1974).

[28]A. Watt, R. P. Singhal, M. H. Storm, and R. R. Whitehead, J. Phys. G **7**, L145 (1981).

[29]P. Anderson, L. P. Ekström, and J. Lyttkens, Nucl. Data Sheets **48**, 251 (1986).

[30]D. J. Weber, G. M. Crawley, W. Benenson, E. Kashy, and H. Nann, Nucl. Phys. **A313**, 385 (1979).

[31]D. Evers, W. Assmann, K. Rudolph, S. J. Skorka, and P. Sperr, Nucl. Phys. **A230**, 109 (1974).

[32]J. A. Cameron, private comnunication of some elements of the Ph.D. thesis of R. Schubank, McMaster University.

[33]M. R. Bhat, Nucl. Data Sheets **51**, 95 (1987).

[34]A. D. Efimov, K. I. Erokhina, V. G. Kiptilyi, I. Kh. Lemberg, V. M. Mikhailov, and B. I. Rzhanov, Izv. Akad. Nauk SSSR, Ser. Fiz. **48**, 10 (1984).

[35]L. Cleemanns, U. Eberth, J. Eberth, W. Neumann, and V. Zobel, Phys. Rev. C **18**, 1049 (1978).

[36]M. R. Bhat, Nucl. Data Sheets **55**, 1 (1988).

[37]T. Paradellis and C. A. Kalfas, Phys. Rev. C **25**, 350 (1982).

[38]A. P. de Lima, A. V. Ramayya, J. H. Hamilton, B. Van Nooijen, R. M. Ronningen, H. Kawakami, R. B. Piercey, E. de Lima, R. L. Robinson, H. J. Kim, L. K. Peker, F. A. Rickey, R. Popli, A. J. Caffrey, and J. C. Wells, Phys. Rev. C **23**, 213 (1981); **23**, 2380 (1981).

[39]M. E. Barclay, L. Cleemann, A. V. Ramayya, J. H. Hamilton, C. F. Maguire, M. C. Ma, R. Soundranayagam, K. Zhao, A. Balanda, J. D. Cole, R. B. Piercy, Amand Faessler, and S. Kuyucak, J. Phys. G **12**, L295 (1986).

[40]L. Cleemann, J. Eberth, W. Neumann, N. Wiehl, and V. Zobel, Nucl. Phys. **A334**, 157 (1980).

[41]R. Soundranayagam, R. B. Piercey, A. V. Ramayya, J. H. Hamilton, A. Y. Ahmed, H. Yamada, C. F. Maguire, G. L. Bomar, R. L. Robinson, and H. J. Kim, Phys. Rev. C **25**, 1575 (1982).

[42]P. Andersson, L. P. Ekström, and J. Lyttkens, Nucl. Data Sheets **39**, 641 (1983).

[43]L. P. Ekström and J. Lyttkens, Nucl. Data Sheets **38**, 463 (1983).

[44]R. L. Auble, Nucl. Data Sheets **28**, 559 (1979).

[45]N. J. Ward and J. K. Tuli, Nucl. Data Sheets **47**, 135 (1986).

[46]J. N. Mo and S. Sen, Nucl. Data Sheets **39**, 741 (1983).

[47]F. Kearns and N. J. Ward, Nucl. Data Sheets **35**, 101 (1982).

[48]A. P. de Lima, J. H. Hamilton, A. V. Ramayya, B. van Nooi-

jen, R. M. Ronningen, H. Kawakami, R. B. Piercey, E. de Lima, R. L. Robinson, H. J. Kim, W. K. Tuttle, L. K. Peker, F. A. Rickey, and R. Popli, Phys. Lett. **83B**, 43 (1979).

[49]K. J. Weeks, C. S. Han, and J. P. Draayer, Nucl. Phys. **A371**, 19 (1981).

[50]B. Sherril, K. Beard, W. Benenson, B. A. Brown, E. Kashy, W. E. Otrand, H. Nann, J. J. Kahayias, A. D. Bacher, and T. E. Ward, Phys. Rev. C **28**, 1712 (1983).

[51]J. Görres, T. Chapuran, D. P. Balamuth, and J. W. Arrison, Phys. Rev. Lett. **58**, 662 (1987).